Segmented Lung CT Image Refinement Through Hybrid Edge-Preserving De-Noising and Variance-Regulated Adaptive Histogram Equalization

T. Bhuvaneshwari, Rohini Pinapatruni
Department of Computer Science and Engineering,
Faculty of Science and Technology (ICFAI Tech),
ICFAI Foundation for Higher Education, Hyderabad, India

***Abstract*—Lung diseases are detected effectively by Chest CT Medical images. Chest CT images are 3D, and they are used for detecting abnormalities in the lungs like pneumonia, tuberculosis, tumors, etc. Chest CT images suffer from different types of noise. The presence of various types of noise, such as Gaussian noise, Quantum noise, and salt-and-pepper noise, will reduce the quality of the image. The noise that is present in CT images may not affect radiologist to diagnose the disease, but it will definitely affect AI-based systems in predicting the disease. Noise occurs because of reduced radiation, insufficient photon information, errors during image reconstruction, and fluctuations in imaging system components. In this work, to improve the quality of Chest CT images, two algorithms are proposed. The first algorithm, Adaptive Edge Preserving Hybrid De-Noising Framework (AEPH) for Segmented Lung CT Images, is used to detect and reduce Noise. The second algorithm, Variance Regulated Adaptive Histogram Equalization (VRAHE), is proposed for improving de-noising and contrast enhancement performance in segmented lung CT images. At first, lung regions are segmented from the LIDC-IDRI dataset. The segmented Chest CT images are converted to 2D CT slices. These 2D CT slices are binary lung-segmented images. These are converted to lung mask images. Random noise models are added only in the lung regions to preserve the background information without modification. The proposed work, AEPH, is applied to reduce noise. The main goal of AEPH is to reduce noise without modifying structural details and edge-related details. Experiments are conducted on a workstation computer with NVIDIA RTX GPU support. When compared to proposed AEPH to conventional approaches in removing noise from CT images, it is identified that AEPH is more effective than conventional methods. The metrics used for evaluating the proposed noise removal approach AEPH when compared to existing approaches are PSNR, SSIM, EPI, RMSE, and entropy, and the values achieved are 32.96 dB, 0.934, 0.93, 9.84, and 7.12, respectively. After de-noising, the second proposed algorithm, VRAHE, successfully improved the image quality by enhancing contrast distribution and preserving important local information. The improved performance was evaluated using CNR, AMBE, UIQI, and EME metrics. From the experimental results, the values achieved are 5.96, 3.14, 0.972, and 31.48, respectively. The Results proved that the proposed work, AEPH, reduced noise, and VRAHE improved contrast levels in segmented lung CT images. The final chest CT images resulting from applying the proposed algorithms maintain brightness and also show the regional lung details more clearly.**

Keywords*—*Chest CT Images; lung segmentation; medical image denoising; adaptive edge preserving hybrid filter; variance regulated adaptive histogram equalization; VRAHE; contrast enhancement; low-dose CT; noise suppression

I. Introduction

The CT scan is a 3D medical image used for investigating diseases related to the lungs. The CT Scan machine captures the internal structure of the human body in the form of sectional images, also called slices. X-rays are 2D images, but they are primarily used to find whether there is an abnormality or not. If an abnormality is found, then the patient is advised to go for a CT scan for further investigation. CT scans, when compared with regular chest X-ray, it gives more information about lung regions. Minor changes in tissues, nodules, infections, and damaged areas can be identified clearly from the CT images. This is the primary reason why doctors use CT scans for identifying diseases like lung cancer, COVID 19, pneumonia, fibrosis, and other lung problems. Nowadays, researchers are applying machine learning and deep learning models to CT scan images for doing automatic analysis. These models are mainly developed to separate lung regions, identify abnormal portions, classify infected areas, and predict different diseases. The LIDC-IDRI is a popular dataset that is used by many research works for lung nodule identification and other CT image-related experiments [17].

Despite the advantages of chest CT imaging, image quality degradation remains a major challenge during acquisition and low-dose scanning procedures. Different types of noise such as Gaussian noise, quantum noise, and salt and pepper noise may affect the visibility of lung structures and reduce diagnostic quality. Several researchers proposed denoising approaches based on CNN, Transformer, Noise2Noise, and hybrid deep learning methods for improving low-dose CT image quality [1], [3], [4]. Similarly, contrast enhancement and histogram equalization methods were introduced to improve local visibility, edge information, and brightness preservation in medical images [8], [12], [15]. Enhancement techniques can improve visualization of fine anatomical structures and may support better segmentation and classification performance. However, excessive smoothing during denoising or over-enhancement during histogram equalization may remove important clinical details and introduce intensity distortion in lung CT images.

From previous studies, it is identified that many researchers mainly concentrated on either removing noise or improving image quality separately. Only a few works focused on segmented lung regions and maintaining structural information during both processes. Most of the traditional enhancement methods are applied on the complete image without considering the intensity changes present in different lung areas. This problem motivated the development of an Adaptive Edge Preserving Hybrid De-Noising Framework and Variance Regulated Adaptive Histogram Equalization method for segmented lung CT images. The proposed method mainly concentrates on reducing noise present inside the lung regions and also maintaining edge details. It also improves the local contrast without disturbing important anatomical information. The developed method improves the quality of segmented lung CT images, which can be further used for abnormality detection and other medical image processing tasks.

II. Related Works

Computed Tomography (CT) scan is an important medical imaging technique used for identifying and analysing lung-related diseases, mainly COVID-19 and other lung abnormalities. However, CT images are affected by different types of noise that are added during image capturing, transmission, and the low-dose scanning process. These noises decrease the quality of images and also affect the analysis done by doctors and automatic disease classification models. Ashwini and Ramashri developed Noise2Noise (N2N) and Noise2Void (N2V) based denoising methods for COVID-19 CT and chest X-ray images affected with Gaussian, Speckle, and Salt and Pepper noises [1]. In their work, they showed that Noise2Void gives better results for removing different types of noise in CT images, whereas Noise2Noise works better mainly for Gaussian noise removal. The performance of these methods was measured by using PSNR and SSIM values. The authors also explained the importance of maintaining image structures while removing noise. This study shows that deep learning-based denoising methods can improve the quality of medical images without the need for original clean images.

Improving the quality of medical images is not only useful for better viewing but also helps in proper disease identification. Xia et al. studied the effect of denoising techniques on COVID-19 CT image quality by using a pneumonia detection-based framework [2]. In their work, anisotropic diffusion and total variation denoising methods were used, and their effect on classification accuracy was tested with a CNN-based COVID-19 classifier. Their results showed that after removing noise from CT images, the disease detection performance was improved even though normal quality measuring parameters like PSNR and MSE were not showing better values in all cases. This work is important because it explains the relation between the noise removal process and disease identification performance. Similarly, Zhang et al. developed a denoising method by combining Transformer and CNN models for low-dose CT images [3]. Their model used the local feature extraction ability of CNN and the learning ability of Transformer for understanding image information. The proposed method improved PSNR, SSIM, and RMSE values and also maintained the structural details better when compared to normal CNN-based methods. This study explained that protecting small anatomical details is very important while removing noise from medical images.

Recent studies have also focused on denoising low-dose CT images without requiring clean target images. Sawada et al. developed a Noise2Noise-based CNN framework integrated with Channel Attention and Spatial Attention mechanisms for low-dose CT denoising [4]. Their approach utilized only noisy image pairs during training and demonstrated improved PSNR performance compared to standard SRResNet architectures. The study highlighted that attention mechanisms help preserve edge information and important anatomical structures while suppressing noise. Furthermore, the authors showed that denoising using only noisy data is practical in medical imaging scenarios where clean ground-truth CT images are difficult to obtain. These studies collectively indicate that modern denoising approaches should not only remove noise but also preserve clinically significant structures, texture information, and disease-related patterns. Such findings provide strong motivation for developing adaptive enhancement and residual noise suppression techniques specifically for segmented lung CT images.

Several researchers focused on improving medical image contrast and visibility using histogram equalization and adaptive enhancement techniques. Riadi et al. [8] proposed a CLAHE-based contrast improvement method combined with Otsu thresholding for enhancing medical X-ray images. Their work showed that adaptive histogram equalization can improve visibility of important anatomical regions without excessive intensity distortion. Similarly, Rahmi-Fajrin et al. [9] applied wavelet transform and CLAHE techniques for dental X-ray image enhancement and reported improved image clarity and structural visibility. These studies indicate that adaptive contrast enhancement methods are effective for improving local details and visual quality in medical images while preserving important structural information.

Image enhancement and machine learning techniques are used by many researchers for improving abnormality detection in medical chest images. Abdussalam et al. [11] studied different enhancement techniques like gamma correction, BCET, histogram equalization, and CLAHE for improving the quality of chest X-ray images before applying classification. Their work showed that enhancement methods improve the visibility of features and also increase the classification performance, mainly when they are combined with the Support Vector Machine (SVM) classifier. In this study, SVM obtained better Area Under the Curve (AUC) values when compared with Naïve Bayes and Random Forest methods. This shows that SVM is more effective for medical image classification-related work.

Koonsanit et al. [12] developed an improved enhancement method called N CLAHE for digital chest X-ray images. In their method, a normalization technique was combined with CLAHE for improving the local contrast and visibility of structures like lungs and chest regions. The authors identified that normal enhancement methods may increase noise or create an unnatural appearance in the images. However, their proposed hybrid enhancement method provided better contrast and improved the visualization quality. Their results showed the importance of adaptive local enhancement techniques for maintaining important structural details in radiographic images used for diagnosis and screening processes.

Many researchers have worked on medical image enhancement using different preprocessing and contrast improvement techniques. MRI and X-ray image processing methods have shown the importance of preserving image quality during enhancement [5], [6]. Histogram-based enhancement methods, adaptive gamma correction, and adaptive histogram equalization have also been widely used to improve contrast while maintaining important structural information [7], [13], [14], [16]. Similar approaches were applied for chest X-ray image enhancement and noise reduction before further image analysis and disease identification [10]. These studies indicate that effective enhancement methods should improve image quality without affecting the important anatomical details.

An image reconstruction network using CNN is proposed in [18]. An adversarial image reconstruction network and an enriched deep residual network are proposed for image retrieval, which gave better results [19],[20]. A refined residual network using a pretrained network is applied on medical image databases in [21]. Various deep learning models in the medical domain are presented in [22].

III. METHODOLOGY

The proposed work introduces an Adaptive Edge Preserving Hybrid De-Noising Framework and a Variance Regulated Adaptive Histogram Equalization (VRAHE) approach for improving segmented lung CT image quality. The denoising framework is designed to suppress Gaussian, quantum, and salt-and-pepper noises while preserving important edge and structural details inside segmented lung regions. The proposed VRAHE method further improves local contrast, brightness preservation, and visibility of anatomical structures without producing excessive intensity distortion. The major novelty of this work lies in performing region-focused denoising and adaptive enhancement specifically on segmented lung CT regions, which helps preserve important clinical details while improving overall image quality for further abnormality analysis and diagnostic applications.

The detailed architecture is shown in Fig. 1. The proposed work used the LIDC-IDRI chest CT dataset containing 1018 patient CT volumes. Each patient scan is processed using a 3D U-Net model to identify and separate the lung region from the remaining thoracic structures. The detailed training configuration details used for segmentation are shown in Table I below. The segmentation network generates a binary lung mask for every CT volume, where lung pixels are retained while non-lung regions are excluded. These binary masks are then applied to the corresponding CT volumes to obtain segmented three-dimensional lung images containing only the lung anatomy. Since the subsequent image enhancement algorithms operate on individual CT slices, the segmented 3D lung volumes are converted into two-dimensional lung CT slices. These segmented lung slices are used as the input for the proposed Adaptive Edge Preserving Hybrid De-Noising Framework (AEPH), followed by the Variance Regulated Adaptive Histogram Equalization (VRAHE) method for improving image quality.

The proposed work takes lung-segmented masked CT images as input. Where the lung region is obtained by applying the binary lung mask on the original CT slices. Gaussian noise, quantum noise, and salt-and-pepper noise are considered in the region of interest, and the Adaptive Edge Preserving Hybrid De-Noising Framework performs noise removal using local variance estimation, edge preservation, and adaptive noise suppression. Hybrid filtering with weighted fusion is applied to reduce residual noise while maintaining lung edges and structural information. The de-noised lung slice is again processed using Variance Regulated Adaptive Histogram Equalization for contrast regulation, brightness preservation, and local detail enhancement to get the final refined lung CT slice. Algorithm 1 on Adaptive Edge Preserving Hybrid De-Noising Framework for Segmented Lung CT Images and Algorithm 2 on Variance Regulated Adaptive Histogram Equalization (VRAHE) are given in the section below.

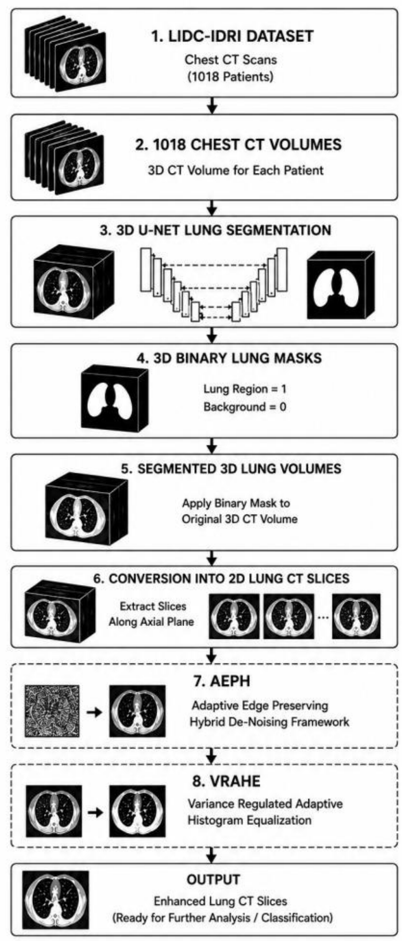

Fig. 1. Proposed architecture – AEPH and VRAHE for improving chest CT.

TABLE I. TRAINING CONFIGURATION OF 3D UNET

Parameter	Configuration
Dataset	LIDC-IDRI chest CT dataset (1018 CT volumes)
Dataset Split	70% Training, 15% Validation, 15% Testing
Network Architecture	3D U-Net with encoder-decoder structure and skip connections

Parameter	Configuration
Input / Output	Input: 3D chest CT volumes; Output: 3D binary lung masks
Computing Platform	Ubuntu Server, Intel Core i7, 32 GB RAM, NVIDIA RTX GPU (12 GB) with CUDA support

The detailed parameter configuration used for AEPH algorithms is shown in Table II below.

TABLE II. PARAMETER CONFIGURATION OF PROPOSED AEPH

Parameter	Configuration
Local Analysis Window	5 × 5 pixels
Adaptive Median Filter Window	Variable (3 × 3 to 7 × 7)
Guided Filter Radius	4 pixels
Adaptive Fusion Strategy	Variance-based weighted fusion

Algorithm-1: Adaptive Edge Preserving Hybrid De-Noising Framework for Segmented Lung CT Images

1. Input Segmented Noisy Lung CT Image

Let the segmented noisy lung CT image be.

$$I(x,y) \quad (1)$$

where, x,y represent pixel coordinates and I(x,y) represents intensity value

2. Lung-Region-Aware Local Mean Estimation

For each sliding local window W,

only valid lung-region pixels are considered.

Local mean is computed as.

$$mu_W=\frac{1}{N_L}\sum_{(i,j)\in W_L} I\,(i,j) \quad (2)$$

where, W_L represents valid lung pixels inside the local window, N_L represents the number of valid lung pixels inside the local window, mu_W represents the local mean intensity.

3. Lung-Region-Aware Local Variance Estimation

Local variance is computed only using valid lung pixels.

$$\sigma_W^2=\frac{1}{N_L}\sum_{(i,j)\in W_L}(I(i,j)-mu_W)^2 \quad (3)$$

where, σ_W^2 represents local variance.

4 . Impulse Noise Density Estimation

$$D_W=\frac{N_{impulse}}{N_L} \quad (4)$$

where, D_W represents impulse noise density, $N_{impulse}$ represents the number of impulse-noise pixels.

5. Impulse Noise Detection Condition

$$D_W>T_d \quad (5)$$

where, T_d represents the impulse noise threshold.

6. Edge Strength Estimation

$$G(x,y)=\sqrt{G_x^2+G_y^2} \quad (6)$$

where, $G(x,y)$ represents edge strength at pixel (x,y), G_x represents horizontal gradient, G_y represents vertical gradient.

7. Adaptive Median Filtering

Impulse-noisy regions are denoised using adaptive median filtering.

$$I_m(x,y)=median\left(W_{xy}\right) \quad (7)$$

where, $I_m(x,y)$ represents the median-filtered image output, W_{xy} represents the local neighborhood window centered at (x,y).

8. Guided Filtering

Gaussian noisy regions are denoised using guided filtering.

$$I_g(x,y)=a_k I(x,y)+b_k \quad (8)$$

where, $I_g(x,y)$ represents the guided filtered output image, a_k represents the local linear coefficient, b_k represents the bias coefficient.

9. Wavelet Transform

$$W=WT(I) \quad (9)$$

where, W represents coefficients, and WT(I) represents the wavelet transform operation applied to image I.

10 . Wavelet Thresholding

$$W_T=0 \text{ if } |(W)|<\lambda$$

$$W_T=W-\lambda \text{ if } |(W)|\geq\lambda$$

where, W_T represents thresholded wavelet coefficients, λ represents the threshold value.

11. Non-Local Means Filtering

$$I_{nlm}(x)=\sum_{y\in\omega} w\,(x,y)I(y) \quad (10)$$

where, $I_{nlm}(x)$ represents the non-local means filtered image, ω represents the search region, $w(x,y)$ represents the similarity weight.

12. Similarity Weight Computation

Similarity weights are computed as.

$$w(x,y)=\frac{1}{Z(x)}exp\left(\frac{-\left(P(x)-P(y)\right)^2}{h^2}\right) \quad (11)$$

where, $P(x)$ represents the image patch centered at pixel x, $P(y)$ represents the image patch centered at pixel y, h represents the normalization factor, $Z(x)$ represents normalization factor.

13. Adaptive Weighted Fusion

Outputs from all denoising filters are combined as.

$$I_f=w_1 I_m+w_2 I_g+w_3 I_w+w_4 I_{nlm} \quad (12)$$

where, I_f represents the adaptively fused denoised image and w_1, w_2, w_3, w_4 represent adaptive fusion weights, I_w represents the wavelet-denoised image.

14. Weight Constraint

Adaptive weights satisfy.

$$w_1+w_2+w_3+w_4=1 \quad (13)$$

This is to ensure normalized adaptive fusion

15. Adaptive Weight Selection

Adaptive weights are dynamically selected using.

$$w_i = f(\sigma_W, G, D_W) \tag{14}$$

where, w_i represents the adaptive weight for each denoising filter.

16. Edge Preservation Factor

Edge-preservation control factor is computed as

$$\alpha(x,y) = e^{-G(x,y)} \tag{15}$$

where, $\alpha(x,y)$represents edge-preservation coefficient.

17. Final Edge-aware Reconstruction

The final denoised image is reconstructed as

$$I_{final} = \alpha I_f + (1-\alpha) I \tag{16}$$

where, I_{final} represents the final denoised segmented lung CT image.

The proposed Variance Regulated Adaptive Histogram Equalization (VRAHE) method was developed to improve local contrast and visibility of segmented lung CT images. The method adaptively regulates histogram enhancement based on local variance information to preserve brightness and avoid excessive intensity amplification. The proposed approach improves visualization of anatomical structures and enhances local details while maintaining structural consistency in lung regions. The following Table III shows the parameter configuration of the VRAHE algorithm.

TABLE III. PARAMETER CONFIGURATION OF VRAHE

Parameter	Configuration
Local Processing Window	8 × 8 pixels
Variance Regulation	Local variance-based adaptive regulation
Variance Threshold (T)	Adaptive threshold estimated from local variance
Contrast Enhancement	Local adaptive histogram equalization

Algorithm-2: Variance Regulated Adaptive Histogram Equalization (VRAHE)

1. Input Denoised and Lung Masked Chest CT Image

The denoised chest CT image containing only the segmented lung region is taken as input.

$$I_D(x,y) \tag{1}$$

where, $I_D(x,y)$ is the denoised and lung-masked chest CT image, and x, y are pixel coordinates

2. Division into Local Windows

The lung CT image is divided into small local windows for adaptive processing. Local analysis helps preserve fine pulmonary structures and texture details.

$$W_k = I_D(i,j) \tag{2}$$

where, W_k= and $I_D(i,j)$ are pixel intensity values

3. Local Mean Computation

The local mean represents the average intensity within each local CT region. It provides brightness information for variance estimation.

$$mu_k = (1\%N) \sum I_i \tag{3}$$

where, mu_k is the local mean, N is the total number of pixels, and I_i is pixel intensity.

4. Local Variance Computation

$$\sigma_k^2 = (1\%N) \sum (I_i - mu_k)^2 \tag{4}$$

where, $\sigma_k^2 islocalvariance$, $mu_k islocalmean$, $I_i = pixelintensity$.

5. Variance Regulation Factor Estimation

The enhancement strength is controlled using local variance information. This prevents over-enhancement in smooth regions containing residual noise.

$$R_k = \sigma_k^2 / (\sigma_k^2 + C) \tag{5}$$

where, R_k is the local variance regulator factor. $\sigma_k^2 = localvariance$, C is a small constant

6. Local Histogram Construction

A histogram is generated for each local CT region. It represents the intensity distribution within the local window.

$$H_k(r) = n_r \tag{6}$$

where, $H_k(r)$is the histogram value.

n_r is the gray scale frequency

7. Probability Density Function Computation

Histogram values are normalized to obtain probability density values. This gives the occurrence probability of each intensity level.

$$P_k(r) = n_r \% N \tag{7}$$

where, $P_k(r)$ is the probability density function,n_r is the histogram frequency, and N is the total number of pixels

8. Cumulative Distribution Function Computation

The cumulative distribution function is computed from probability density values. It is used for adaptive histogram equalization transformation.

$$CDF_k(r) = \sum P_k(j) \tag{8}$$

where, $CDF_k(r), P_k(j)$ are the cumulative distribution function and probability density values.

9. Variance Regulated Adaptive Enhancement

Histogram equalization is adaptively controlled using the variance regulation factor. Detailed lung regions receive stronger enhancement than smooth regions.

$$I_E(x,y) = R_k \times CDF_k(r) \times (L-1) \tag{9}$$

where, $I_E(x,y)$ is the enhanced CT image, R_k is the variance regulation factor, and L is the total number of gray levels.

10. Residual Noise Suppression

Low variance regions are controlled using a suppression factor. This prevents amplification of residual noise after denoising.

$$\sigma_k^2 < T ? \left(I_F(x,y) = \alpha \times I_E(x,y) : I_F(x,y) = I_E(x,y)\right) \tag{10}$$

where, $I_F(x,y)$ is the final enhanced image, α is the suppression coefficient, and T is the variance threshold.

11. Final Enhanced Chest CT Image

All enhanced local windows are combined to generate the final enhanced CT image. The output image contains improved contrast and preserved pulmonary structure $I_{VRAHE}(x,y)=I_F(x,y)$ (11)

where, $I_{VRAHE}(x,y)$ is the final enhanced chest CT image, $I_F(x,y)$ is the enhanced image after suppression.

IV. Experimental Results

The Lung Image Database Consortium and Image Database Resource Initiative (LIDC-IDRI) dataset is a publicly available chest CT image dataset used widely in medical imaging research. The dataset contains thoracic CT scan images collected from different hospitals and imaging systems. It includes lung CT images with expert annotations provided by experienced radiologists. The dataset is useful for lung image enhancement, denoising, segmentation, and disease analysis studies. Since the dataset contains large variations in image quality and acquisition conditions, it is suitable for developing and validating image processing algorithms for chest CT images [17]. The detailed dataset description is shown in Table IV.

TABLE IV. Dataset Description

Parameter	Description
Dataset Name	LIDC-IDRI
Imaging Modality	Thoracic Computed Tomography (CT)
Total CT Scans	1018 lung CT scans (130GB, appx 244,000 DICOM image slices)
Annotation Details	Annotated by 4 experienced thoracic radiologists

The chest CT images obtained from the LIDC-IDRI dataset [17] were first processed using lung segmentation. This step was performed to extract only the lung region from the complete chest CT images. Binary lung masks were generated to separate the lung area from unwanted background regions and other structures ash shown in the figure below. The original dataset contains three-dimensional CT volumes. These 3D CT scans were converted into two-dimensional CT image slices for further processing. The generated binary masks were then applied to each 2D CT slice to obtain segmented lung CT images. These segmented images were further used for denoising and image enhancement processes in the proposed work.

The proposed work was implemented on a workstation system running Ubuntu Server operating system with GPU support. The system was configured with an Intel Core i7 processor, 32 GB RAM, and 1 TB SSD storage for CT image processing tasks. NVIDIA RTX GPU with 12 GB of dedicated memory and CUDA support was used for accelerated computation.

The above Fig. 2 and 3 show results after applying 3D UNet to produce a segmented lung mask image and the segmented lung mask with noise (left) and ground truth image without noise (right).

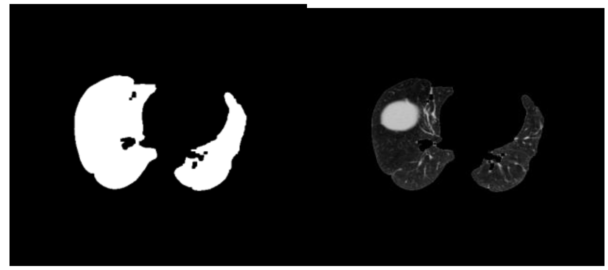

Fig. 2. Segmented lung binary image (Left), segmented lung mask image (Right).

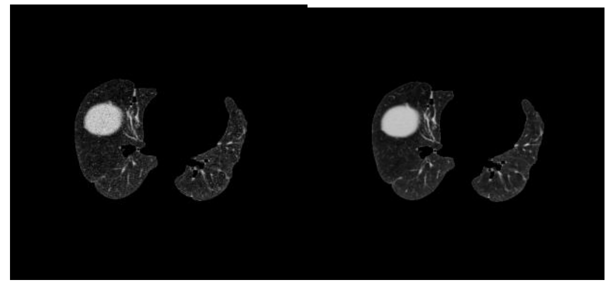

Fig. 3. Segmented lung binary image with Noise (Left), with out Noise (Right).

The performance of the proposed Adaptive Edge Preserving Hybrid De-Noising Framework was evaluated using segmented lung CT images obtained from the LIDC-IDRI dataset. The denoising performance was analyzed using quantitative image quality metrics such as PSNR, SSIM, RMSE, EPI, and Entropy. The obtained results were compared with existing denoising approaches to analyze noise suppression capability and edge preservation performance. The average values of PSNR, SSIM, RMSE, and EPI of all denoised images are calculated and used for comparison purposes. Table V shows the performance analysis of the proposed work.

TABLE V. Performance Analysis of the Proposed Adaptive EDGE Preserving Hybrid De-Noising

Method	PSNR (Mean ± SD)	SSIM (Mean ± SD)	RMSE (Mean ± SD)	EPI (Mean ± SD)	Entropy (Mean ± SD)
Noisy Image	18.42 ± 0.62	0.610 ± 0.050	28.54 ± 0.59	0.420 ± 0.004	5.21 ± 0.015
Median Filter	24.85 ± 0.48	0.790 ± 0.038	17.41 ± 0.46	0.710 ± 0.003	6.01 ± 0.013
Gaussian Filter	25.92 ± 0.42	0.820 ± 0.031	15.63 ± 0.38	0.750 ± 0.003	6.18 ± 0.012
Bilateral Filter	27.14 ± 0.34	0.860 ± 0.024	13.41 ± 0.31	0.810 ± 0.002	6.52 ± 0.011
BM3D	29.85 ± 0.24	0.890 ± 0.016	11.52 ± 0.24	0.860 ± 0.002	6.71 ± 0.010
AEPH	32.96 ± 0.15	0.934 ± 0.030	9.84 ± 0.19	0.930 ± 0.001	7.12 ± 0.0094

Table V shows the quantitative performance comparison of different denoising methods applied to segmented lung CT images. The noisy image produced poor PSNR, SSIM, and EPI values with high RMSE due to the presence of noise and structural degradation. Conventional filtering methods improved the image quality to some extent, but fine edge and texture details were partially affected during noise suppression. The proposed AEPH method achieved better PSNR, SSIM, EPI, and Entropy values with lower RMSE, indicating improved noise removal and preservation of important lung structures.

The following graphs, shown in Figs. 4 -7, compare the denoising performance using PSNR, SSIM, RMSE, and EPI metrics, respectively. The proposed AEPH achieved the highest PSNR and SSIM values, along with the lowest RMSE and highest EPI. These results show that AEPH provides better noise removal while preserving important edge and structural details than the existing denoising methods.

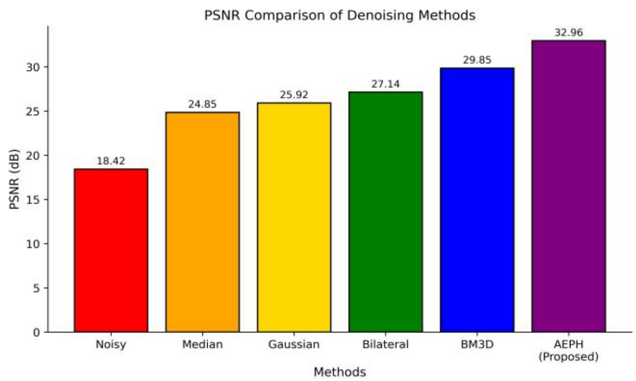

Fig. 4. PSNR comparison of denoising methods.

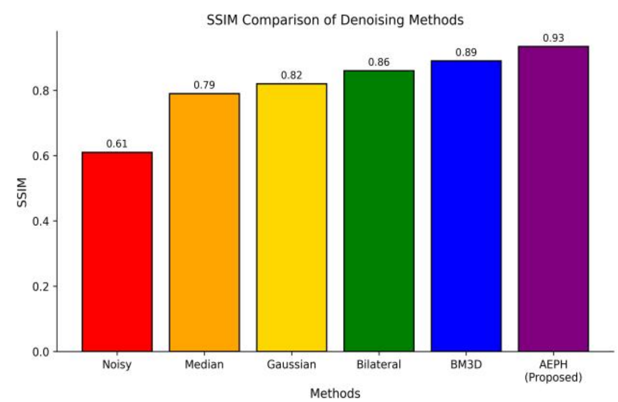

Fig. 5. SSIM comparison of denoising methods.

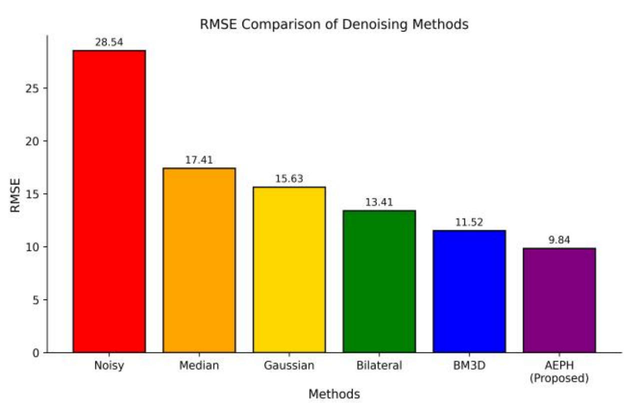

Fig. 6. RMSE comparison of denoising methods.

After implementation of Algorithm 1, Adaptive Edge-Preserving Hybrid Denoising Framework for Segmented Lung CT Images, the denoised images are input to the second algorithm, Variance Regulated Adaptive Histogram Equalization (VRAHE), to improve the contrast of the image. The VRAHE algorithm was evaluated using segmented lung CT images from the LIDC-IDRI dataset. The enhancement performance was analyzed using CNR, AMBE, UIQI, and EME metrics. These metrics were used to evaluate contrast improvement, brightness preservation, and local detail enhancement. The obtained results were compared with conventional histogram equalization methods. The details are shown in Table VI, and the lung segmented before and after applying VRAHE is shown in Fig. 8.

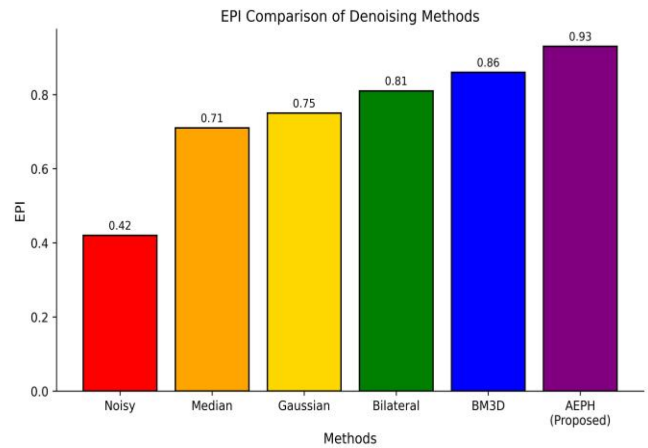

Fig. 7. EPI Comparison of denoising methods.

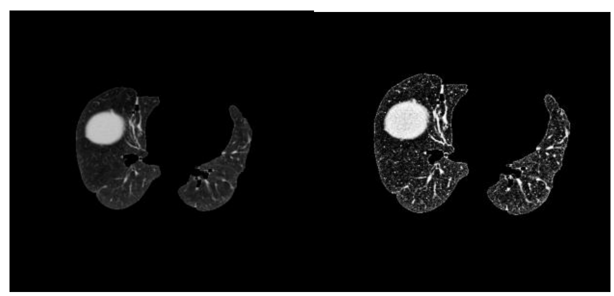

Fig. 8. Before (L) and after (R) applying VRAHE.

TABLE VI. QUANTITATIVE PERFORMANCE ANALYSIS OF VRAHE ENHANCEMENT METHOD

Method	CNR (Mean ± SD)	AMBE (Mean ± SD)	UIQI (Mean ± SD)	EME (Mean ± SD)
Original Image	2.14 ± 0.18	16.82 ± 0.62	0.741 ± 0.020	11.26 ± 0.95
HE	3.08 ± 0.15	11.34 ± 0.51	0.826 ± 0.015	16.72 ± 0.81
CLAHE	4.12 ± 0.12	7.26 ± 0.39	0.901 ± 0.010	22.84 ± 0.66
VRAHE (Proposed)	5.96 ± 0.08	3.14 ± 0.18	0.972 ± 0.004	31.48 ± 0.42

An ablation study was carried out to study the role of the major stages in the proposed AEPH and VRAHE framework. AEPH reduced noise using adaptive filtering, guided filtering, wavelet denoising, and adaptive fusion, and obtained a PSNR of 32.96 dB, SSIM of 0.934, and RMSE of 9.84. After denoising, VRAHE improved contrast and brightness preservation with CNR of 5.96, AMBE of 3.14, UIQI of 0.972, and EME of 31.48. The results show that each stage adds to the overall refinement of segmented lung CT images. Fig. 9 below shows the Comparative Performance Analysis of Lung CT Image Enhancement Methods.

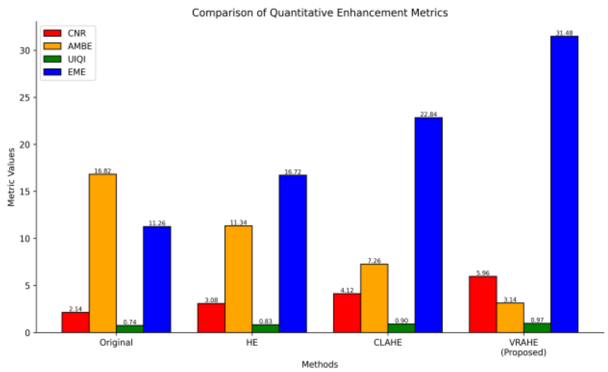

Fig. 9. Comparative performance analysis of lung CT image enhancement methods.

V. Conclusion

This work presented an Adaptive Edge Preserving Hybrid De-Noising Framework for Segmented Lung CT Images and a Variance Regulated Adaptive Histogram Equalization (VRAHE) approach for improving the quality of segmented lung CT images. The proposed denoising framework effectively reduced Gaussian, quantum, and salt-and-pepper noises while preserving important edge and structural information. The obtained results achieved PSNR of 32.96 dB, SSIM of 0.934, EPI of 0.93, RMSE of 9.84, and Entropy of 7.12, indicating effective noise suppression and structural preservation.

The proposed VRAHE method further improved local contrast and visibility of lung structures without producing excessive intensity distortion. Quantitative evaluation produced CNR of 5.96, AMBE of 3.14, UIQI of 0.972, and EME of 31.48, showing improved contrast enhancement and brightness preservation performance. The overall experimental analysis demonstrated that the proposed approaches can effectively improve the quality of segmented lung CT images and preserve important anatomical details useful for further medical image analysis and abnormality detection.

VI. Future Direction

In future work, the proposed Adaptive Edge Preserving Hybrid De-Noising Framework and Variance Regulated Adaptive Histogram Equalization (VRAHE) approach can be extended for real-time clinical applications using GPU-based parallel processing architectures. The proposed methods can also be integrated with deep learning-based abnormality detection and classification models for automated lung disease analysis. Further improvement can be achieved by developing adaptive region-based enhancement methods for preserving fine lesion structures in low-dose CT images. The proposed framework may also be extended to 3D volumetric CT analysis, multimodal medical imaging applications, and explainable AI-assisted diagnostic systems for improved clinical interpretation and decision support.

Acknowledgment

The Research Scholar expresses her sincere thanks to the research supervisor and institution for providing necessary guidance and support to complete this research work. The authors acknowledge the medical image datasets and computational facilities used for carrying out the experiments. The suggestions and encouragement received during the development of the Adaptive Edge Preserving Hybrid DeNoising Framework and Variance Regulated Adaptive Histogram Equalization method helped in improving the overall quality of the proposed work.

References

[1] G. Ashwini and T. Ramashri, “Denoising of COVID-19 CT and chest X-ray images using deep learning techniques for various noises using single image,” in Proc. International Conference on Signal Processing, Computation, Electronics, Power and Telecommunication (IConSCEPT), 2023.

[2] L. Xia, H. Jebbari, O. Deforges, L. Zhang, L. Lévêque, and M. Outtas, “Denoised CT Images Quality Assessment Through COVID-19 Pneumonia Detection Task,” in Proc. 15th International Conference on Quality of Multimedia Experience (QoMEX), 2023.

[3] J. Zhang, Z. Shangguan, W. Gong, and Y. Cheng, “A novel denoising method for low-dose CT images based on transformer and CNN,” Computers in Biology and Medicine, vol. 163, p. 107162, 2023.

[4] S. Sawada, S. Murakami, L. Guangxu, and T. Kamiya, “A Method for Denoising from Low-Dose CT Images Based on Noise2Noise,” in Proc. 23rd International Conference on Control, Automation and Systems (ICCAS), 2023.

[5] T. Haueise, F. Schick, N. Stefan, and J. Machann, “Comparison of the accuracy of commercial two-point and multi-echo Dixon MRI for quantification of fat in liver, paravertebral muscles, and vertebral bone marrow,” European Journal of Radiology, vol. 172, p. 111359, 2024.

[6] Y. Pourasad and F. Cavallaro, “A novel image processing approach to enhancement and compression of X-ray images,” International Journal of Environmental Research and Public Health, vol. 18, no. 13, pp. 1–18, 2021.

[7] S. Senthilkumar and R. Rajesh, “Histogram modification approaches for medical X-ray image enhancement,” International Journal of Computer Applications, vol. 97, no. 12, pp. 20–26, 2014.

[8] A. A. Riadi, E. Wijayanti, W. H. Sugiharto, A. Latubessy, and A. C. Murti, “Automated contrast improvement of X-ray image using Otsu threshold on contrast-limited adaptive histogram equalization algorithm,” in Proc. International Conference on Information and Communications Technology, 2018, pp. 1–6.

[9] H. Rahmi-Fajrin, S. Puspita, S. Riyadi, and E. Sofyan, “Dental digital image enhancement using wavelet and CLAHE approaches,” International Journal of Advanced Computer Science and Applications, vol. 10, no. 5, pp. 112–118, 2019.

[10] M. Sharma and D. Kumar, “Contrast enhancement and noise reduction of chest X-ray images,” in Proc. International Conference on Computational Intelligence and Sustainable Engineering Solutions (CISES), 2022, pp. 570–574.

[11] T. M. Abdussalam, H. A. Nugroho, and I. Soesanti, “Image Enhancement Techniques on Chest X-Ray Images to Improve COVID-19 Detection,” in 2022 4th International Conference on Biomedical Engineering (IBIOMED), Yogyakarta, Indonesia, 2022, pp. 87–90, doi: 10.1109/IBIOMED56408.2022.9987990.

[12] K. Koonsanit, S. Thongvigitmanee, N. Pongnapang, and P. Thajchayapong, “Image Enhancement on Digital X-Ray Images Using N-CLAHE,” in Proceedings of the International Conference on Digital Image Processing and Medical Imaging, Thailand, pp. 1–4.

[13] M. Veluchamy and B. Subramani, “Image contrast and color enhancement using adaptive gamma correction and histogram equalization,” Optik, vol. 183, pp. 329–337, 2019, doi: 10.1016/j.ijleo.2019.02.054.

[14] J. B. Zimmerman, S. M. Pizer, E. V. Staab, J. R. Perry, W. McCartney, and B. C. Brenton, “An evaluation of the effectiveness of adaptive histogram equalization for contrast enhancement,” IEEE Transactions on Medical Imaging, vol. 7, no. 4, pp. 304–312, Dec. 1988, doi: 10.1109/42.14513.

[15] H. Lidong, Z. Wei, W. Jun, and S. Zebin, “Combination of contrast limited adaptive histogram equalisation and discrete wavelet transform for image enhancement,” IET Image Processing, vol. 9, no. 10, pp. 908–915, 2015, doi: 10.1049/iet-ipr.2014.0755.

[16] D.-C. Chang and W.-R. Wu, “Image contrast enhancement based on a histogram transformation of local standard deviation,” IEEE Transactions on Medical Imaging, vol. 17, no. 4, pp. 518–531, Aug. 1998, doi: 10.1109/42.730397.

[17] S. G. Armato III, G. McLennan, L. Bidaut, M. F. McNitt-Gray, C. R. Meyer, A. P. Reeves, B. Zhao, D. R. Aberle, C. I. Henschke, E. A. Hoffman et al., “The Lung Image Database Consortium (LIDC) and Image Database Resource Initiative (IDRI): A completed reference database of lung nodules on CT scans,” Medical Physics, vol. 38, no. 2, pp. 915–931, 2011.

[18] Pinapatruni, R., Shoba Bindu, C. Learning image representation from image reconstruction for a content-based medical image retrieval. SIViP , 1319–1326 (2020).

[19] Pinapatruni, R., Chigarapalle, S.B. Adversarial image reconstruction learning framework for medical image retrieval. SIViP 16, 1197–1204 (2022).

[20] Pinapatruni, R., Chigarapalle, S.B. (2022). EDR: Enriched Deep Residual Framework with Image Reconstruction for Medical Image Retrieval. Computer Vision and Image Processing. CVIP 2021. Communications in Computer and Information Science, vol 1568. Springer.

[21] Pinapatruni, R., Chigarapalle, S.B ,Images reconstruction using a refined Res-UNet model for medical image retrieval,ACTA IMEKO,March 2022,Volume 11.

[22] Pinapatruni, R., Bhuvaneshwari, T. (2025). Deep Learning Innovations for Predictive Healthcare Systems. ICICC 2024. Lecture Notes in Networks and Systems, vol 1241. Springer, Singapore. https://doi.org/10.1007/978-